

# The Escape Gating Technique for a Multiwire Proportional Chamber

Shen Changquan, Shen Peiruo and Ye Zongnan

(Institute of High Energy Physics, Chinese Academy of Sciences, Beijing)

Li Xiaonan

(Department of Physics, Zhengzhou University)

---

A balloon-borne spectrometer for hard X-ray astronomy observation in space has been developed with the escape gating technique. It contains a multiwire proportional chamber filled with high pressure mixture of xenon and methane. In this paper, we will describe the principle of the escape gating technique, the way to realize it in our spectrometer and its practical performance. The spectrometer was set in a balloon and successfully launched to an altitude of 37 km above sea level near Beijing on August 31, 1986. Useful observing data were recorded during the flight.

---

## 1. INTRODUCTION

In recent years, with the further improvement of the carrier vehicles, many new discoveries have been made in the active observations of X-ray and gamma ray astronomy. As in the near earth space the intensities of the X-ray and gamma ray emitted by most of the celestial bodies are very low and the backgrounds in detectors induced by the cosmic ray, X-ray and gamma ray background are much more intense and furthermore, the hard X-ray with the energy higher than 15 keV has a strong

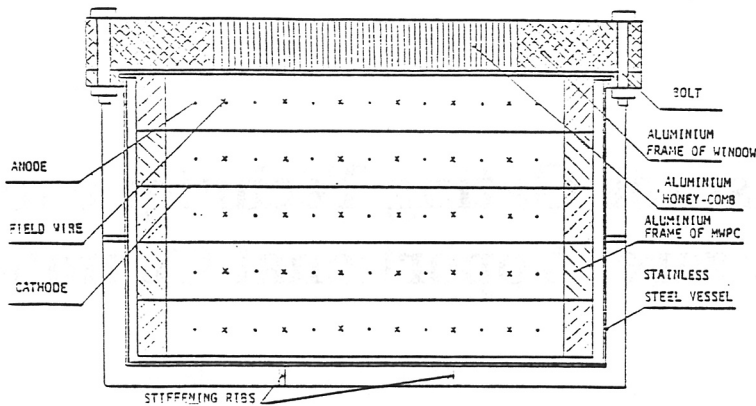


**FIG. 1** Sectional view of a multiwire proportional chamber filled with high pressure xenon.

penetrating power and cannot be focused and imaged as optical rays, an advanced hard X-ray telescope operating in space must have high sensitivity (large sensitive area, high efficiency and low background), excellent energy resolution, light weight (so as to be carried to space easily) and good position resolution (for imaging). The multiwire proportional chamber filled with high pressure xenon (Xe-MWPC) can meet all these requirements, while the escape gating technique (EGT) can further improve the energy resolution and background rejection to make the Xe-MWPC an ideal hard X-ray telescope[1,2,3,].

In order to carry out X-ray astronomy observation on a balloon, we have made such a hard X-ray spectrometer, containing a Xe-MWPC and adopting EGT.

## 2. THE PRINCIPLE OF THE ESCAPE GATING TECHNIQUE

The structure of the Xe-MWPC is shown in Fig.1 and the detailed description can be found in Reference [4]. Inside the pressure vessel, the chamber is separated by 6 cathode planes into 5 layers with a thickness of 3 cm each. The field wires intervene between every two neighbouring anode wires in the same layer. The grounded cathode and field wires divide the chamber into a number of cells. Each cell centers about an anode wire supplied with a high voltage and gas, framing a  $3\text{cm} \times 3\text{cm}$  cross section and just acting as a wallless proportional tube. The chamber is filled with a mixture gas of xenon and methane in the ratio 95:5 at a pressure of 3 atmospheres.

When an incident X-ray photon interacts with an atom of the gas inside the chamber and the deposited energy is larger than the noise threshold, the photon can be detected. The photoelectric effect is dominant in the interaction between xenon atom and X-ray photon with the energy below 200 keV. In this energy range, the interaction of a hard X-ray photon with a small number of  $\text{CH}_4$  atoms can be ignored. When the energy of the incident X-ray photon,  $E_x$ , is greater than the xenon's K-edge energy,  $E_K$ , the mode of its photoelectric interactions is shown in Fig.2 [5,6]. In Fig.2, the processes followed by the vacancy created in L and the outer shells are elaborated, because the fluorescence yields in these shells are small, and even for the L-fluorescent photons with the highest energy, their mean free path is still less than  $0.6\text{ cm}\cdot\text{atm}$ , so they can be taken as being converted into free electrons near their production point, especially in a chamber with so wide a gap and filled with high pressure gas.

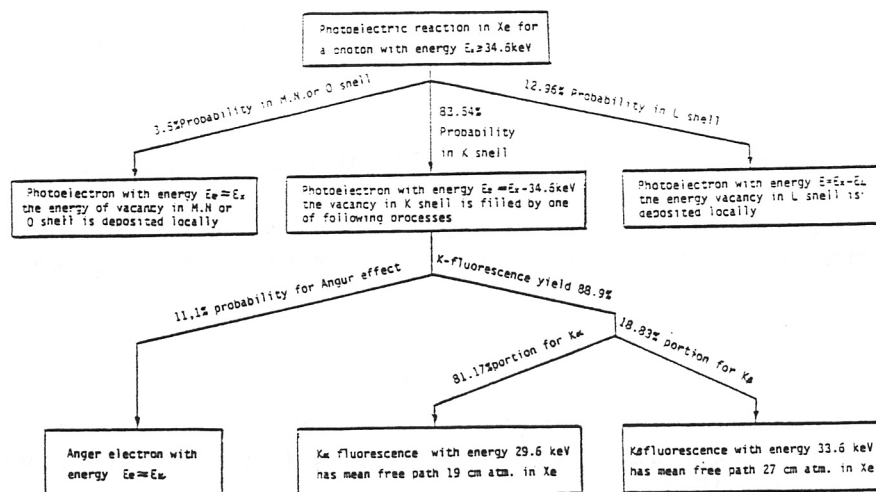


**FIG. 2** All possible processes of photoelectric reaction in xenon for a hard X-ray photon with energy  $E_x > 34.6\text{ keV}$ .

Fig.2 shows that when an incident photon with an energy greater than 34.6 keV interacts with an xenon atom, K-fluorescent photon is generated with the probability of 74.3% ( $83.54\% \times 88.9\%$ ), and the rest of the energy transforms into the kinetic energies of the free electrons (photoelectron or Auger electron) and successively deposits on the spot. A K-fluorescent photon travels some distance in the chamber before being absorbed. Such an event usually deposits energy at two locations. If these two locations are in different cells, signals can be detected simultaneously from two anode wires, and one of them must correspond to the well-known K-fluorescence energy of xenon. Using K-fluorescence signal as a necessary coincidence condition for event selecting is the very principle of the EGT. Other photoelectric processes causing incident photons to lose all the energies near the interaction points are all rejected by EGT. Therefore, the detection efficiency of EGT is limited up to 74.3%. In fact, the efficiency is even lower because some of the K-fluorescence is absorbed inside the cell where the original interaction occurs and some of the K-fluorescence may escape from the chamber, both of them are naturally rejected by EGT. In addition, the efficiency is also affected by the size of the cells and the pressure of xenon. As all these processes are random, the actual detection efficiency of the Xe-MWPC adopting EGT has to be measured through experiments and evaluated by Monte Carlo simulations. Our preliminary results from Monte Carlo simulations are shown in Fig.3. The results were experimentally checked with different radioactive sources. Curve A in Fig.3 is the detection efficiency when EGT is not adopted. In such a case the cells on the sides and bottom of the chamber are only used for anticoincidence. Curve B is the detection efficiency when EGT is adopted. In this case the cells on the sides and bottom of the chamber can be used for anticoincidence but also for opening a 'gate' to the xenon K-fluorescence. This means that if the signal is a fluorescent one, it will be regarded as a detection signal just like the other fluorescent signals rather than an anticoincidence signal so as to increase the detection efficiency of EGT.

Although EGT decreases the detection efficiency of Xe-MWPC, it has two advantages: to improve the energy resolution, and to lower the background. Furthermore, it is not necessary to make a correction for the escape peak in the calculation of the X-ray emitted spectrum from the detected data, thus reducing the error and increasing the reliability in spectrum measurement.

The energy resolution for a MWPC without using EGT is:

$$R = \frac{\Delta E}{E} \quad (1)$$

where  $E$  is the energy of the incident photon,  $\Delta E$  is FWHM of the peak of the energy  $E$  in the detected spectrum.

Since the energy of the Xe K-fluorescence  $E_t$  is precisely known when adopting the EGT, the fluctuation of the signal amplitude of K-fluorescence can be avoided and the energy resolution  $R'$  is

$$R' = \frac{\Delta E_e}{E_e + E_t} = \frac{\Delta E_e}{E} \quad (2)$$

where  $E_e$  is the sum of the energy of photoelectrons and Auger electrons on the outer shells,  $E_t$  is the energy of K-fluorescence. With  $E_e < E$ ,  $\Delta E_e < \Delta E$ , and  $R' < R$ . In this way EGT improves the energy resolution of the Xe-MWPC.

EGT selects a K-fluorescent signal as the trigger condition, while K-fluorescence can only be generated in the photoelectric interactions of hard X-ray. Thus, a great number of background events which cannot generate K-fluorescence can be rejected.

### 3. THE ESCAPE GATING ELECTRONICS

All anodes are divided into 5 groups to simplify the electronics and to shorten the dead time for triggering. The anodes in the same group are connected in parallel to a common preamplifier and a linear amplifier as the input channel of the escape gating circuits. The anodes in the bottom layer and side cells are combined as the fifth group which acts as an anticoincidence shield, the 20 cells in the central part are divided into 4 groups (as shown in Fig.4). The principle of group numbering is to form the neighbouring cells into different groups with the distance between different cells in the same group as far as possible, so as to improve the detection efficiency of the escape gate.

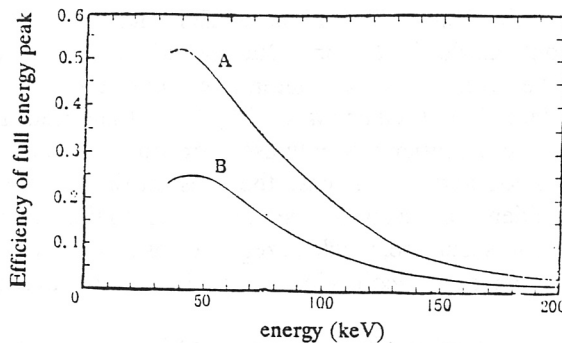


FIG. 3 The detecting efficiency of Xe-MWPC with 3 atm. Curve A corresponds to normal Xe-MWPC. Curve B corresponds to the Xe-MWPC adopting EGT.



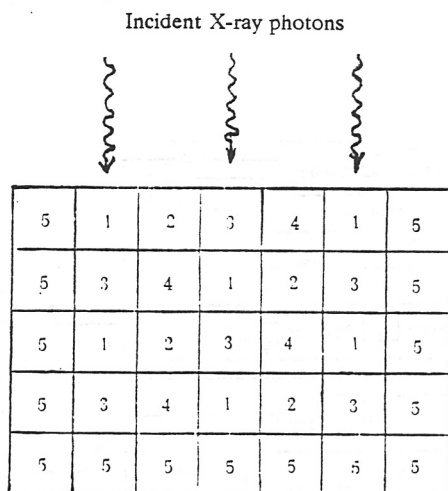


FIG. 4 The scheme of anode wires divided into 5 groups.

Data acquisition is controlled by a microprocessor on board the balloon payload. In order to shorten the dead time of the detector, the output signals from the Xe-MWPC are instantly selected by the hardware of the escape gating circuits. If there is an event selected, the circuits give out a request for an interruption of the CPU, and trigger the corresponding ADC to do A-D conversion.

The microprocessor on board the balloon uses Z80 as the CPU, and adopts the STD bus and block structure. It offers the trigger level 2 and handles the events in the detector by means of interruption.

Fig.5 is a block diagram of the escape gating circuits. Only the fourth and the fifth channel are given in the diagram, the omitted parts (the first, the second and the third) are just the same as the fourth one.

The output signal of the amplifier in each channel feeds a noise discriminator and a single channel analyser which discerns the K-fluorescence by its amplitude. In the first channel to the fourth one, when a K-fluorescent photon is detected, the single channel analyser in the corresponding channel is triggered and generates an inner-gate signal, which prevents the sampler in the same channel from being triggered, results in zero reading of the ADC in this channel and adds one count in the fluorescence counter. In such a way, the microprocessor adds the accurate value of the K-fluorescent energy to the total energy of the detected photon. A signal triggering the noise discriminator but not the single channel analyser is called an outer-gate signal, which triggers the sampler and ADC in the same channel to do A-D conversion.

The preamplifier, amplifier, noise discriminator and single channel analyser in the fifth channel are the same as in other channels. But the outer-gate signal in the fifth channel acts as an anticoincidence signal, which prevents the circuits from requesting an interruption, discharges all capacitors in the peak keepers and samplers, clears the fluorescence counter and resets all circuits in 15 microseconds. The inner-gate signal in the fifth channel plays the same role as in other channels instead of anticoincidence. In this way, more fluorescence is detected and the efficiency of EGT is improved.

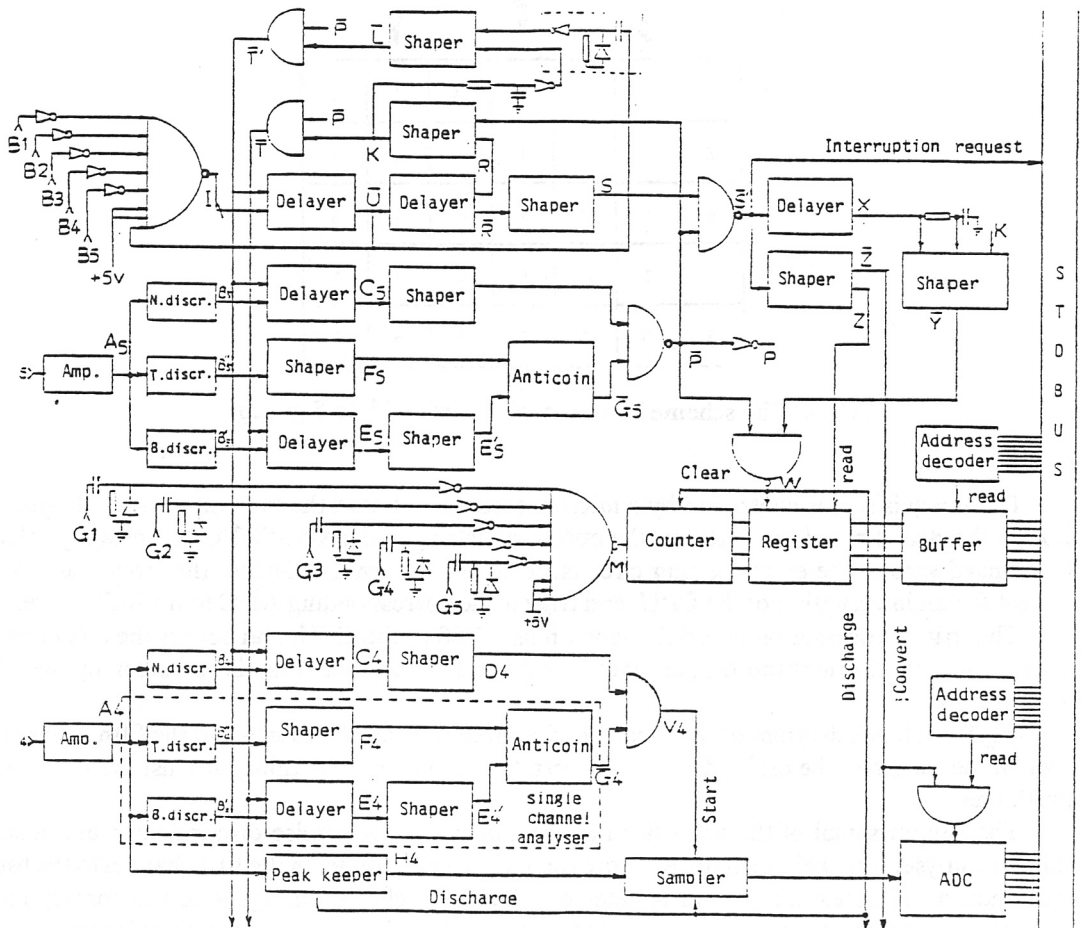
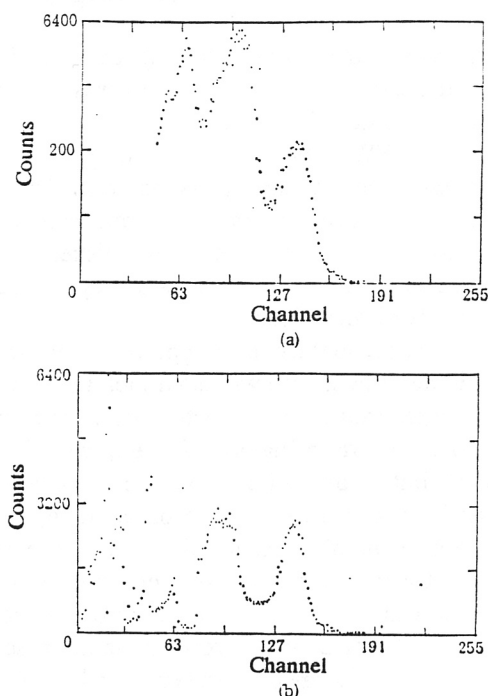


FIG. 5 The block diagram of the escape gating circuits.

The inner-gate signal in all channels and the outer-gate signal in the first, second, third or fourth channels can start the interruption request and turn the escape gating circuits into an insensitive state to input, until the microprocessor on board the balloon finishes processing the event with the interruption subroutine, discharge processes of all capacitors in the peak keepers and



**FIG. 6** The measured  $^{57}\text{Co}$  spectra with Xe-MWPC.

Fig.6(a) is the "normal spectrum". Fig.6(b) is the "good spectrum".

samplers are finished and the fluorescence counter and all ADC are cleared. Such an event expends 82 microseconds as dead time.

When the interruption subroutine is operated by the microprocessor on board the balloon, first the count  $n$  in the fluorescence counter is multiplied by the number corresponding to K-fluorescent energy  $E_f$  of xenon, then the product and output values of all ADC are accumulated and the sum of them corresponds to the total energy  $E$  of the events, at last one count is increased in the corresponding channel of the spectra. If  $n \geq 1$  or  $E < 34.6$  keV, the event is counted into the "good spectrum". If  $n = 0$  and  $E > 34.6$  keV, the event is counted into the "normal spectrum" which is not valid for EGT. The events with energy  $E > 200$  keV are counted into the highest channel No. 255 of the corresponding spectrum.

#### 4. PERFORMANCE AND DISCUSSIONS

Our escape gating Xe-MWPC was tested with the radioactive sources of  $^{57}\text{Co}$ ,  $^{241}\text{Am}$  and  $^{133}\text{Ba}$ . Fig.6 is the measured energy spectrum of  $^{57}\text{Co}$ . The peak on the right side is the full energy peak of the strongest gamma ray line (122 keV).

In Fig.6, the unit of abscissa is 'channel', the value of energy calibration is 0.88 keV/channel. Fig.6(a) is a "normal spectrum", where there is an escaping peak which is higher in counts than the total energy peak and corresponds to the energy of 92 keV. This peak results from the events of the Xe K-fluorescence photons escaping from Xe-MWPC. Another peak, the peak of tungsten fluorescence, appears at 59 keV. As there is a lot of tungsten wires in the chamber, the fluorescence

yield in the photoelectric interactions of hard X-ray with tungsten is as high as 95.7%. Most of the tungsten fluorescent photons would escape from the tungsten wires and would be absorbed by Xe in the MWPC resulting in a peak of tungsten K-fluorescence.

In Fig.6(a), the energy resolution (FWHM) of the total energy peak of 122 keV is about 22%, but in Fig.6(b) (the "good spectrum") the 122 keV peak narrows down apparently, the energy resolution is 13%. This shows that the escape gating technique can really improve the energy resolution of Xe-MWPC. In Fig.6(b) the escape peak diminishes, which helps improve the observation precision of the emitted spectrum of the celestial X-ray sources and helps increase the reliability of the hard X-ray astronomy observations.

Since the  $^{57}\text{Co}$  radioactive source used in the energy spectrum measurement was too strong, we adopted a lead collimator, and shielded the source with some lead plates. As a result, two lead K-fluorescent peaks emerged in the measured energy spectra, which is represented by a peak with double tops around channel 89--97 as shown in Fig.6(b). In fact, there is also a contribution from such a lead fluorescence in Fig.6(a), but it cannot be seen since it is covered by the 92 keV escape peak which has similar energy and more counts. On the other hand, as EGT is adopted, some photoelectrons whose energy is close to one of the xenon K-fluorescence energies may be mistaken for fluorescence. This causes the distortion of the energy spectrum around 30 keV and 60 keV as shown in Fig.6(b). This is the disadvantage of EGT. This distortion range can be reduced by improving the energy resolution of Xe-MWPC and narrowing the fluorescence 'gates' of the single channel analysers in the circuits. Since the energy of X-ray emitted by  $^{241}\text{Am}$  is just in the distortion range of the energy spectrum, its energy spectrum measured with EGT is not shown and its energy resolution is calculated with formula (2).

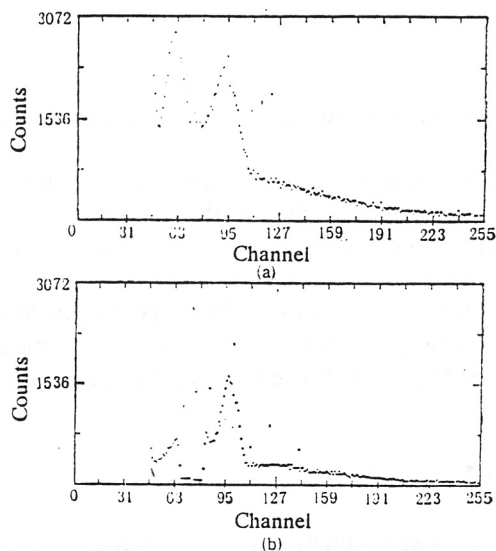


FIG. 7 The measured  $^{133}\text{Ba}$  spectra with Xe-MWPC. Fig.7(a) is the "normal spectrum". Fig.7(b) is the "good spectrum".

Fig.7 is the measured energy spectrum of  $^{133}\text{Ba}$  with the main contribution from the 81 keV photons.  $^{133}\text{Ba}$  has many hard X-ray and gamma ray lines emitted, which broaden the peaks and raise the ground lines in the spectra, giving the impression that the background is very high.

The measurement in the laboratory shows that the energy resolution of the Xe-MWPC adopting EGT is higher than 13% in the energy range of 35--122 keV, better suited in higher energy range. With the energy difference between  $K_{\alpha}$  fluorescence and  $K_{\beta}$  fluorescence of Xe being about 4 keV, the above-mentioned escape gating circuits open only one 'gate' and the central energy corresponds to weighted average value of  $K_{\alpha}$  and  $K_{\beta}$ , 30.4 keV. If we open the 'gate' and register the counts for  $K_{\alpha}$  and  $K_{\beta}$  respectively, the energy resolution can be further improved. In addition, the dead time of the detector can also be reduced if we upgrade the capability of the analog processing power in the escape gating circuits to shorten the time required for processing events in the balloon-borne microprocessor.

This hard X-ray spectrometer was set in a balloon with a volume of 120,000 m<sup>3</sup> and launched to the space of 37 km high at the Xianghe Balloon Station, Hebei Province, China on August 31, 1987. A successful observation was carried out and a great quantity of useful data were obtained. The whole payload was safely recovered early the next morning. Observation data are now being processed.

#### ACKNOWLEDGMENTS

The authors are indebted to Prof. Lu Zhuguo, Prof. Meng Lie, Prof. Sun Yaoguo and Prof. Huo Anxiang for their support and help. We would like also to thank Miss Kong Minnan for designing some circuit elements, and to Mr. Li Yi and Miss Wang Hongjuan for taking part in some work.

#### REFERENCES

- [1] P. Ubertini et al., *Nucl. Instr. & Meth.* 217(1983)97.
- [2] G. Bibbo and P. W. Sanford, *Nucl. Instr. & Meth.* 179(1981)189.
- [3] D. P. Sharma et al., 20th International Cosmic Ray Conference Vol. OG 9, 1--3 (August 2--15, 1987, Moscow).
- [4] Shen Changquan et al., Nuclear Techniques and Its Applications in Science Research, Industry, Medicine and Agriculture (Chinese Journal), Vol. 10 (1987) No. 6, 5.
- [5] F. Saull, "Principles of Operation of Multiwire Proportional and Drift Chambers" CERN 77-09 3rd MAY 1977.
- [6] E. F. Plechaty et al., "Tables and Graphs of Photon Interaction Cross Sections from 1.0 keV to 100 MeV Derived from LLL Evaluated Nuclear Data Library" (1975) UCRL-50400 Vol. 6, Rev. 1.
- [7] Ye Zhongnan and Shen Changquan, "A Data Acquisition System of the Space Hard X-ray Spectroscope", Nuclear Electronics and Detection Technology (Chinese Journal) Vol. 9 (1989), No. 1, 54.